

# UC Santa Barbara

## UC Santa Barbara Previously Published Works

### Title

Interaction of adsorbed polymers with supported cationic bilayers

### Permalink

<https://escholarship.org/uc/item/909794mw>

### Journal

RSC Advances, 3(43)

### ISSN

2046-2069

### Authors

Das, Saurabh  
Donaldson, Stephen H  
Kaufman, Yair  
[et al.](#)

### Publication Date

2013

### DOI

10.1039/c3ra43500h

### Copyright Information

This work is made available under the terms of a Creative Commons Attribution-NonCommercial License, available at <https://creativecommons.org/licenses/by-nc/4.0/>

Peer reviewed

## Interaction of adsorbed polymers with supported cationic bilayers†

Cite this: DOI: 10.1039/c3ra43500h

Saurabh Das, Stephen H. Donaldson Jr., Yair Kaufman and Jacob N. Israelachvili\*

The interaction forces between bilayers of the cationic surfactant di(tallow ethyl ester)dimethyl ammonium chloride (DEEDMAC) were measured using a Surface Forces Apparatus (SFA) with and without an adsorbing polymer, polyacrylamide (PAM). In the absence of PAM, the forces measured between the bilayer surfaces were purely repulsive on approach and separation and is charge regulated. Addition of PAM induced structural changes to the bilayer interfaces, and resulted in the formation of bilayer-like patches of DEEDMAC decorated PAM (hydrated) on the mica surface. The interaction potential between these surfaces showed a modified DLVO interaction with an additional monotonic steric hydration repulsion on approach with an exponential force decay length of  $D_{\text{steric}} \sim 1$  nm consistent with the measurements of hydration forces. On separating the surfaces, interdigitated polymers bridge between the two surfaces, resulting in a weak adhesion (adhesion energy,  $W_0 \sim 0.1$  mJ m<sup>-2</sup>). Our results provide a picture of the complex molecular structure and interactions between uncharged adsorbing water soluble polymers and supported charged bilayers, and highlight the effects of adsorbing polymers on the structure of bilayers. Implications for the stability of vesicles in dispersions have been also discussed.

Received 10th July 2013  
Accepted 21st August 2013

DOI: 10.1039/c3ra43500h

www.rsc.org/advances

### Introduction

Supported bilayers have received considerable attention as models for cell membranes, for their ability to bio-functionalize inorganic and polymeric surfaces, immobilize proteins on surfaces and provide nanometer thick insulating layers on conductive surfaces.<sup>1,2</sup> These properties make supported bilayers ideal candidates for protein receptor biosensors.<sup>3,4</sup> Supported bilayers can also serve as a model system in order to study cell membranes and functions of various cellular organs.<sup>1,5-7</sup> The interfacial properties of vesicles and lipid bilayers can be altered by adsorbing proteins<sup>8</sup> and adsorption of bio-molecules at membrane surfaces determines the biophysical, biochemical and mechanical properties of cell membranes.<sup>9,10</sup>

A significant amount of work has been done to understand the process of vesicle fusion at solid interfaces, a mechanism by which the vesicles adhere, and subsequently, crowding and vesicle stresses lead to the formation of a continuous supported bilayer on different kinds of surfaces.<sup>11-16</sup> The combined effects of solution conditions, vesicle properties and surface properties on the formation of supported bilayers from vesicles have been explored previously.<sup>12</sup> However, the addition of polymers in vesicle dispersions and the effects of polymeric additives on the

interactions between vesicle surfaces have yet to be thoroughly examined experimentally.

Charged vesicles in dilute solution interact through attractive van der Waals forces and repulsive electrostatic forces, together known as the Derjaguin–Landau–Verwey–Overbeek (DLVO) theory. DLVO theory can describe the interaction between vesicles in a dilute solution.<sup>17-19</sup> However, in a concentrated dispersion in the presence of polymer additives, no simple theory can accurately determine the interaction between vesicles. In the presence of *adsorbing* or *non-adsorbing* polymers, combined effects due to DLVO forces, steric repulsion, depletion attraction, hydration and hydrophobic forces, and forces due to mechanical deformation of the vesicle surface may all contribute to the overall interaction potential.

The addition of polymers to vesicle dispersions significantly alters the forces of interaction between the vesicles, and can ultimately result in phase instability and aggregation of the vesicles. This undesirable effect is often encountered in various consumer products such as detergents and fabric softeners, which contain concentrated vesicle dispersions along with other additives such as perfumes, dyes and polymers.<sup>20</sup> An understanding of the surface properties, *e.g.*, the surface charge and potential of the vesicles and how these parameters change due to adsorbed and non-adsorbed polymers, is essential to determine the stability and phase behavior of the vesicles. The effect of uncharged adsorbing and non-adsorbing polymers on vesicle stability has been studied theoretically.<sup>21-25</sup> However, no experimental measurements on the forces between the vesicles were made.

Department of Chemical Engineering, University of California, Santa Barbara, CA 93106, USA. E-mail: jacob@engineering.ucsb.edu

† Electronic supplementary information (ESI) available. See DOI: 10.1039/c3ra43500h

Supported bilayers have been used before as a model system in order to simulate and determine vesicle interactions in solution.<sup>19</sup> The effect of *non-adsorbing* charged and uncharged polymers on the forces between bilayers were explored experimentally.<sup>19</sup> Simulation of polymer grafted lipid bilayers were performed<sup>26</sup> and experimental evidence of hydrophobic interaction between the protein molecules and lipid domains were investigated by X-ray diffraction technique.<sup>8</sup> The latter work showed that proteins and polymers adsorb to bilayer surfaces and causes an increase in the head group area of the lipid molecules while collapsing the thickness of the bilayer membrane, still maintaining the bilayer integrity. However, the effect of *strongly adsorbing* polymers due to the hydrophobic interactions on the stability of supported bilayers remains unexplored.

In this paper, we investigated the effect of a *strongly adsorbing* uncharged polymer, polyacrylamide (PAM), on the structure and interaction forces between DEEDMAC bilayers supported on the mica surfaces. Here we show that the interaction forces between the bilayers obey constant charge DLVO theory for bilayer–bilayer separation distance  $D > 4$  nm in a 4.5 mM  $\text{CaCl}_2$  solution at pH 4. For  $D < 4$  nm, the bilayer head groups showed an intermediate behavior between constant charge and constant potential surfaces due to charge regulation during approach and separation of the surfaces. Atomic Force Microscopy (AFM) scans show that PAM tends to adsorb to the bilayer surfaces through hydrophobic interactions and induces structural changes forming bilayer like patches of DEEDMAC decorated PAM on the mica surface. The interaction potential between these surfaces measured in the Surface Forces Apparatus (SFA) showed a modified DLVO interaction with an additional monotonic steric hydration repulsion with an exponential force decay length of  $\sim 1$  nm consistent with the measurements of hydration forces.<sup>27</sup>

## Materials and methods

The cationic surfactant di(tallow ethyl ester) dimethyl ammonium chloride (DEEDMAC) was provided by Procter and Gamble Co (see Fig. 1a). The polymer polyacrylamide (PAM, mol. wt  $\sim 5$ –6 MDa) was obtained from Sigma-Aldrich. A solution of 0.5 wt% of PAM was prepared in a buffer solution of 4.5 mM  $\text{CaCl}_2$  at pH 4 adjusted with concentrated hydrochloric acid. All the solutions were prepared in Milli-Q® water.

### Preparation of the supported cationic bilayers

Bilayers of the cationic surfactant DEEDMAC were deposited on freshly cleaved mica surfaces by Langmuir–Blodgett (LB) technique (Nima Technology). The DEEDMAC surfactant in chloroform ( $1 \text{ mg mL}^{-1}$ ) was injected at the air–water (buffer solution) interface in an LB trough. The mica surfaces immersed in the buffer solution were pulled out of the DEEDMAC layer (at the buffer solution–air interface) into the air phase at a constant surface pressure of  $\Pi = 42 \text{ mN m}^{-1}$  (head group area of the surfactant molecule  $a_0 \sim 55 \text{ \AA}^2$ , see Fig. S1†) to deposit a monolayer of DEEDMAC on the mica surfaces. The DEEDMAC coated mica surface was then slowly immersed back into the buffer solution from the air phase to deposit another monolayer

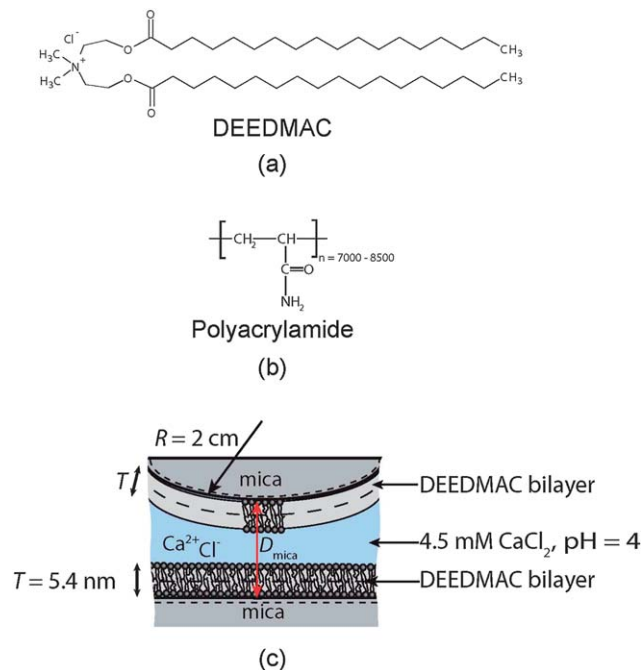


**Fig. 1** (a) The DEEDMAC surfactant deposited on the mica surfaces to form the bilayers. (b) Polyacrylamide polymer of mol. wt 5–6 MDa. (c) Schematics of the surface geometry used in the SFA experimental setup showing the bilayer supported on the mica surfaces. Bilayers of the supported DEEDMAC surfactant were deposited on both mica surfaces in the SFA. For clarity purposes, the surfactant has been illustrated as a shaded grey region for the top mica surface.

of the surfactant resulting in the formation of supported DEEDMAC bilayers. The bilayers adhered to the mica surface through Coulombic interactions between the positively charged DEEDMAC head groups and the negatively charged mica surface. The supported cationic bilayers on the mica surface were kept immersed in the buffer solution over the whole course of the experiment in order to avoid damage due to exposure to air.

### Langmuir–Blodgett (LB) trough experiments

The interaction of the polymer (PAM, mol. wt 5–6 MDa) with the DEEDMAC monolayers spread at the air–water interface was studied in a LB trough. The DEEDMAC surfactant was spread on a clean sub-phase of 4.5 mM  $\text{CaCl}_2$  at pH 4 and held at constant pressure of  $42 \text{ mN m}^{-1}$  while a 0.5 wt% solution of the PAM dissolved in 4.5 mM  $\text{CaCl}_2$  at pH 4 (vol = 50 mL) was injected carefully into the sub-phase (vol = 1.3 L) outside of the trough barriers so as not to disturb the DEEDMAC monolayer. The polymer was then allowed to diffuse throughout the aqueous sub-phase of the trough and interact with the surfactant film for  $\sim 48$  h, after which isotherms of the DEEDMAC monolayer adsorbed at the air–water interface were performed. It should be noted that in the LB trough experiments, the concentration of PAM in the trough was  $\sim 13$  times less than that used for the SFA experiments (*i.e.* 0.5 wt%). Thus, the LB isotherms should be considered as a qualitative tool to determine the effect of PAM on the DEEDMAC molecules adsorbed at the air–water interface.

## Atomic Force Microscope (AFM)

Images were acquired using MFP-3D-Bio AFM (Asylum Research) using BL-AC40TS probe (Asylum Research) in tapping mode at room temperature ( $22 \pm 1$  °C). The DEEDMAC bilayers were prepared on mica using LB trough as described above and scanned in a 4.5 mM CaCl<sub>2</sub> buffer solution at pH 4. In order to study the effect of PAM on the bilayer, the buffer solution was replaced by a 0.5 wt% PAM (prepared in the same buffer solution) and the sample was scanned again.

## The Surface Forces Apparatus (SFA)

The interaction energies,  $W(D)$ , between the supported cationic bilayers were measured in a surface forces apparatus (SFA). Force measurements by SFA have been described elsewhere.<sup>28</sup> Briefly, the normal forces of interaction between two mica surfaces in a cross-cylindrical geometry were measured as a function of the mica–mica separation distance,  $D$ , as measured by multiple beam interferometry (MBI)<sup>28</sup> with angstrom (Å) level distance resolution. The normal force,  $F$ , between two surfaces in cross cylinder geometry (radius of curvature,  $R$ ) can be translated into the energy of interaction between two equivalent flat surfaces by the Derjaguin approximation,<sup>29</sup>  $W(D) = F/2\pi R$ . Before depositing the DEEDMAC bilayers on the mica surfaces, mica–mica contact was measured by the SFA in dry air in order to get the reference distance,  $D = 0$ . The radius of curvature,  $R$ , of the contact point was measured from the shape of the fringes obtained by MBI.<sup>29</sup> The normal force,  $F$  and  $D$  were measured simultaneously at each data point during the experiment. The normal force of interaction between the surfaces,  $F$ , was measured at an approach and separation speeds of 1–3 nm s<sup>-1</sup>. The SFA was filled with the buffer solution before transferring the supported bilayers into the apparatus. The buffer solution was degassed for ~2 h before the experiment to avoid the nucleation of air bubbles during the course of the experiment.

## Results and discussion

### Interaction forces between the supported DEEDMAC bilayers in a 4.5 mM CaCl<sub>2</sub> solution (pH 4) with no polyacrylamide measured in the SFA

The energy of interaction,  $W$ , measured between the two DEEDMAC bilayers supported on the mica surfaces were monotonically repulsive with a force decay length  $D_0 = 3.5$  nm (Fig. 2). A steric hard wall of  $10.8 \pm 0.5$  nm was measured when the bilayer surfaces were brought under hard compression ( $P \sim 100$  MPa). This ‘hard wall’ ( $2T = 10.8$  nm) is equal to twice the bilayer thickness ( $T = 5.4$  nm) supported on the mica surfaces (Fig. 2 and 3). The surface topography of the supported bilayer on the mica surface was visualized with an AFM and is discussed in the AFM section later. The bilayers are in the solid ordered state (frozen) at room temperature (25 °C) since the chain melting temperature,  $T_m$ , of the DEEDMAC surfactant is ~55 °C (private communication with Mansi Seth at UCSB and P&G) and hence hemi-fusion was never observed even at a compressive pressure above  $P \sim 100$  MPa. The energy of

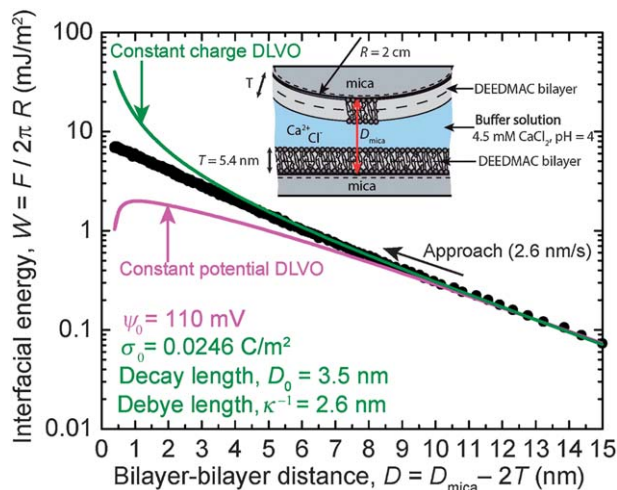


**Fig. 2** Forces measured between the DEEDMAC bilayers on approach in a 4.5 mM CaCl<sub>2</sub> solution at pH 4. The solid green and the magenta line shows the constant charge and constant potential DLVO fits respectively to the measured forces (black solid circles) using the parameters shown in the figure.

interaction between the bilayers was fitted to DLVO theory using both constant surface charge and constant surface potential boundary conditions. DLVO interactions arise as a consequence of an attractive van der Waals force and repulsive electrostatic double layer force between the two surfaces. The van der Waals energy between the two supported bilayer surfaces is given by<sup>29</sup>

$$W_{\text{vdW}} = \frac{F_{\text{vdW}}}{2\pi R} = -\frac{1}{12\pi} \left( \frac{A_{232}}{D^2} - \frac{A_{123}}{(D+T)^2} + \frac{A_{121}}{(D+2T)^2} \right) \quad (1)$$

where  $A_{123}$  is the Hamaker constant for media 1 and 2 interacting across medium 3,<sup>29</sup>  $D$  is the separation distance between the two bilayer surfaces, and  $T$  is the thickness of the bilayers. In these experiments, media 1, 2 and 3 are mica, bilayer and water respectively, and the values for the Hamaker constants are  $A_{232} = 8.0 \times 10^{-21}$  J,  $A_{123} = 3.3 \times 10^{-21}$  J and  $A_{121} = 8.5 \times 10^{-21}$  J.

The electric double layer interaction between two similar surfaces under a constant surface potential,  $\psi_0$ , can be expressed as<sup>30</sup>

$$W_{\psi} = \frac{F_{\psi}}{2\pi R} = \frac{2\kappa\epsilon\epsilon_0\psi_0^2}{1 - e^{-2\kappa D}} (-e^{-2\kappa D} + e^{-\kappa D}) \quad (2)$$

where  $\psi_0$  is the surface potential (of each of the two symmetric surfaces),  $\epsilon$  and  $\epsilon_0$  are the dielectric constant of the liquid and dielectric permittivity of vacuum respectively and  $\kappa$  is the Debye–Hückel parameter and is given by<sup>29</sup> eqn (3) at 25 °C for 2 : 1 electrolytes.

$$\kappa^{-1} = \frac{0.176}{\sqrt{[\text{CaCl}_2]}} \quad (3)$$

where  $[\text{CaCl}_2]$  is in mol L<sup>-1</sup> and  $\kappa^{-1}$  is in nm. In this work,  $[\text{CaCl}_2] = 4.5 \times 10^{-3}$  mol L<sup>-1</sup>. Hence, the Debye length (inverse of the Debye–Hückel parameter,  $\kappa$ ) is  $\kappa^{-1} = 2.6$  nm at 25 °C.

The electric double layer interaction between two similar surfaces under a constant surface charge,  $\sigma_0$ , is given by<sup>31</sup>

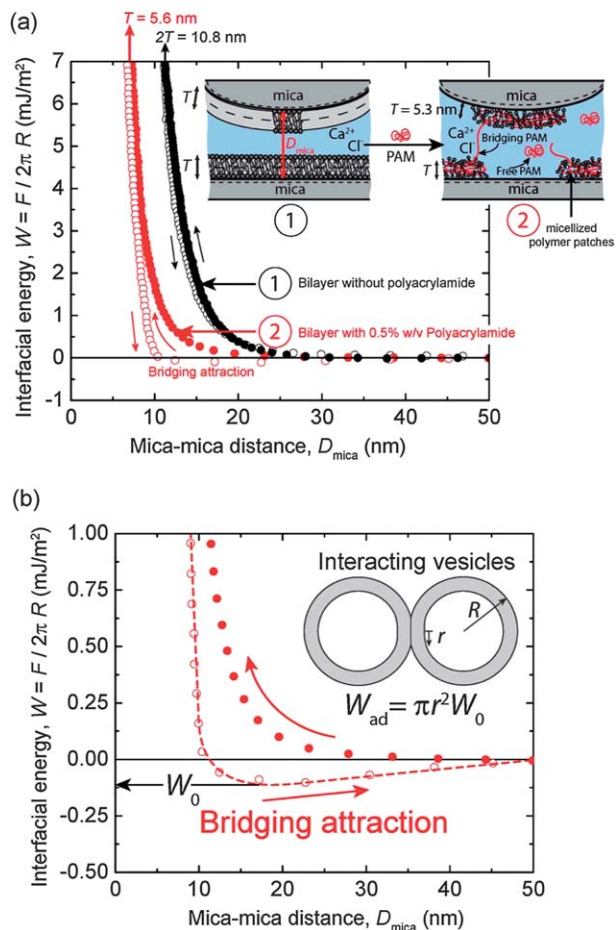


**Fig. 3** (a) Forces measured between the DEEDMAC bilayers on approach (red solid circles) and separation (red open circles) in a 4.5 mM  $\text{CaCl}_2$  solution at pH 4 with 0.5 wt% polyacrylamide between the surfaces. For comparison, the forces measured between the bilayers in the same buffer solution without the polymer is shown in black circles. (b) Same data as in (a) on a magnified force axis to illustrate the effect of PAM on the forces between the bilayers. The inset shows two interacting vesicles that cohere with energy of  $W_{\text{ad}}$  due to the bridging attraction caused by the polymer chains.

$$W_{\sigma} = \frac{F_{\sigma}}{2\pi R} = \frac{2\kappa\epsilon\epsilon_0\psi_0^2}{1 - e^{-2\kappa D}} (e^{-2\kappa D} + e^{-\kappa D}) \quad (4)$$

The surface charge density at 25 °C can be calculated from the Grahame equation and is given by<sup>29</sup>

$$\sigma_0 = 0.117 \sinh(\psi_0/51.4) \sqrt{[\text{CaCl}_2]} \quad (5)$$

where  $\psi_0$  is in mV and  $[\text{CaCl}_2]$  is in  $\text{mol L}^{-1}$ .

It should be noted that eqn (2) and (4) are the approximate solutions to the linearized Poisson–Boltzmann's equation for the two boundary conditions of constant surface potential and constant surface charge respectively. For a real system, neither of these conditions is obeyed and the exact electrostatic interaction energies between surfaces can be determined by minimizing the free energy of the system.<sup>32</sup>

At large separation ( $D > 4$  nm) between the bilayer surfaces, the electrostatic force agrees well with the constant charge DLVO theory (Fig. 2). However, for distances below 4 nm, the

interaction shows an intermediate behavior between the two limits of constant charge and the constant potential DLVO interaction. The bilayer surfaces behave like a charge regulated system, where the surface charge is regulated by the dissociation of the counterion (chloride ion,  $\text{Cl}^-$ ).<sup>32,33</sup> The degree of dissociation of the charged head groups is influenced by the electric field disturbance due to the overlapping electric double layers of the two surfaces and it takes time for the charged head groups to reach chemical equilibrium with the counterions.

Given enough time for equilibration (on the order of 10–30 s)<sup>19</sup> at a given distance, the counterion  $\text{Cl}^-$  near the surface will adsorb to the positively charged DEEDMAC head groups of the bilayer thus reducing the net charge on the surface and resulting in a lower energy of interaction between the surfaces; in this case the force decay length,  $D_0$ , equals the Debye length,  $\kappa^{-1}$ . In these experiments, the surfaces approach dynamically (at a rate of 2.6  $\text{nm s}^{-1}$ ), and the charged head groups are unable to equilibrate with the counterions. The charge regulation results in a higher charge density on the bilayer surfaces, causing a net higher energy of interaction between them. This is evident from the higher value for the measured force decay length ( $D_0 = 3.5$  nm) unlike 2.76 nm (close to  $\kappa^{-1} = 2.6$  nm) observed previously<sup>19</sup> when the surfaces were brought close together quasi-statically giving enough time for the counterion exchange with the bilayer head groups.

#### Interaction forces between the supported DEEDMAC bilayers in a 4.5 mM $\text{CaCl}_2$ solution (pH 4) with 0.5 wt% polyacrylamide (PAM) measured in the SFA

The force of interaction between the DEEDMAC coated mica surfaces in presence of 0.5 wt% PAM were monotonically repulsive and electrostatic in nature with  $D_0 = 3.5$  nm (Fig. 4) on approach, *i.e.*, the same decay length as that between the two bilayer surfaces in the absence of polymer. An extra hydration force (repulsive) was recorded over and above the electrostatic

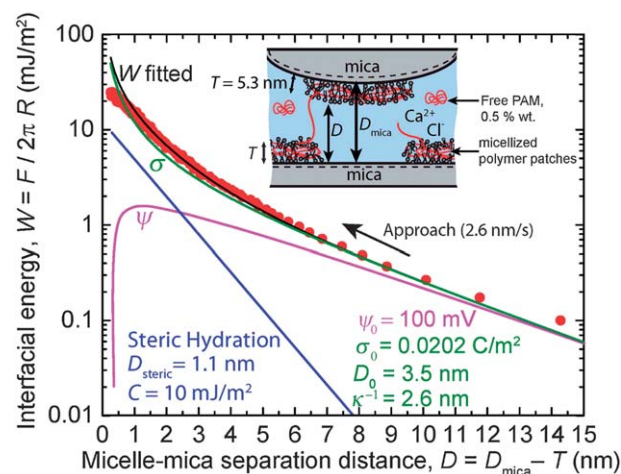


**Fig. 4** Forces measured between the DEEDMAC bilayers on approach in a 4.5 mM  $\text{CaCl}_2$  solution at pH 4 with 0.5 wt% polyacrylamide between the surfaces. The solid green line is the constant charge DLVO (eqn (4)) fit and the solid magenta is the constant potential DLVO (eqn (2)) fit to the experimental data (red solid circles). The solid black line ( $W$  fitted) is the combined constant charge DLVO and the steric hydration force (eqn (6)) fit to the experimentally measured forces.

repulsion (Fig. 4) for  $D < 4$  nm and is given by an empirical equation for steric forces<sup>29</sup> expressed as

$$W_{\text{steric}} = \frac{F_{\text{steric}}}{2\pi R} = Ce^{-\frac{D}{D_{\text{steric}}}} \quad (6)$$

where  $C$  is typically  $3\text{--}30 \text{ mJ m}^{-2}$ ,<sup>27</sup> and  $D_{\text{steric}}$  is the decay length for the hydration forces and is about  $1 \text{ nm}$ .<sup>27</sup> This hydration repulsion is due to the adsorbed layer of water molecules on the hydrophilic domains of the polymer–DEEDMAC patches. The bound water tends to increase the excluded volume of the polymer and hence the steric and the hydration force are intimately connected. On separating the surfaces, an adhesion of about  $W_0 = 0.1 \text{ mJ m}^{-2}$  was measured and is due to bridging attraction<sup>34,35</sup> caused by the PAM chains protruding out of the DEEDMAC–PAM aggregates on the mica surface (Fig. 3a and b). This adhesive force of interaction between the bilayer–polymer aggregates can be used as a tool to understand the stability of vesicles in a polymeric dispersion.

The attractive energy due to the bridging interaction between two adhesive and flattened vesicles can be expressed as

$$W_{\text{ad}} = \pi r^2 W_0 \quad (7)$$

where  $W_0$  is the bridging energy per unit area and  $r$  is the contact radius between the two interacting vesicles (Fig. 3b).

If we consider two interacting vesicles with a radius of curvature of  $R = 1 \mu\text{m}$  (Fig. 3b), with a contact radius of  $r = 0.05$

$\mu\text{m}$  (assuming contact radius to be 5% of  $R$ ), the attractive energy of interaction between them due to bridging forces is  $W_{\text{ad}} = 0.8 \text{ mJ}$ , *i.e.*,  $6 \times 10^4 kT$  ( $k$  = Boltzmann's constant). Interacting vesicles in a dispersion can get trapped into an adhesive well if the adhesion energy is greater than the thermal energy of the dispersion,  $kT$ . Here, the adhesion energy is four orders of magnitude greater than the thermal energy and hence will result in aggregation and phase separation of the vesicles in a polymeric dispersion.

The structural changes to the supported bilayers due to the adsorbed polymer were investigated with AFM. The AFM images (Fig. 5) show that the bilayer was ruptured by the PAM forming small pools of micellized polymers on the mica surface of thickness  $T \sim 6 \text{ nm}$ . This is similar to the final hard wall thickness measured between the mica surfaces when the PAM was injected between the bilayer surfaces. The amide group of the PAM results in a weak hydration repulsion and hence the observed forces were a bit more repulsive than pure electrostatic forces (Fig. 4). The excess repulsion could also be attributed to the overlapping bilayer like patches of DEEDMAC decorated PAM on the mica surfaces getting pushed out when the opposing surfaces are brought into close contact.

This result combined with the below AFM results indicate that PAM adheres to the bilayer through hydrophobic interactions, also resulting in an increase in the head group area of the surfactant molecules in the bilayer (see the LB trough section

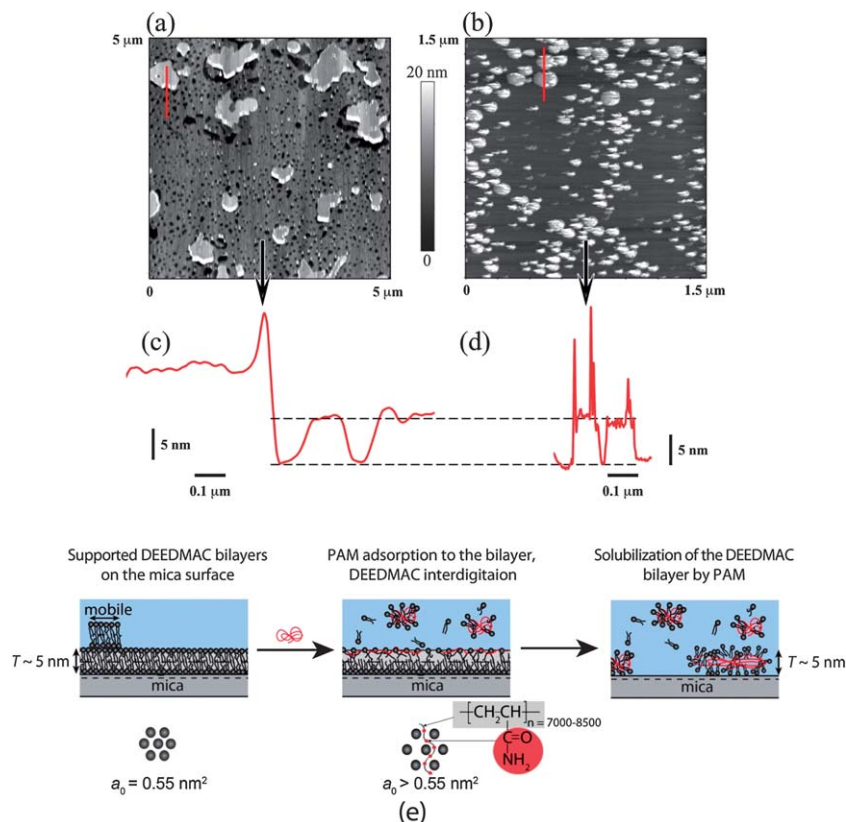


**Fig. 5** (a) AFM topography images of DEEDMAC on mica in  $4.5 \text{ mM CaCl}_2$ . (b) The same sample in  $4.5 \text{ mM CaCl}_2$  with PAM ( $0.5 \text{ wt\%}$ ). (c) and (d) show the cross sections corresponding to (a) and (b) respectively. (e) The mechanism of removal (and micellization) of the supported DEEDMAC bilayer from the mica surface.

below). This increase in the head group area causes inter-digitations of the DEEDMAC hydrocarbon tails and finally causes them to engulf and decorate the PAM surface. This surfactant decorated polymer adheres to the negative charged mica surface through electrostatic interactions, a mechanism similar to the adhesion of the supported bilayers on the mica surfaces.

### Atomic Force Microscope (AFM)

AFM was used to characterize the DEEDMAC topography on the mica surfaces in a 4.5 mM CaCl<sub>2</sub> buffer at pH 4. The DEEDMAC surfactant self-assembled to ~6 nm thick bilayer with several holes and portions of a second bilayer on top (Fig. 5a and c). These patches of second bilayer are mobile and get pushed out of the contact when the surface are brought under compression in the SFA and hence did not affect the hard wall thickness during the force measurements and is consistent with previous observations.<sup>36</sup>

Replacing the buffer solution with 0.5 wt% PAM solution (in the same buffer solution) resulted in rupture of the bilayer, leaving small (~100 nm) patches of PAM–bilayer complex of thicknesses similar to that of a single supported bilayer (Fig. 5b and d). PAM adsorbs to the bilayer surfaces through hydrophobic interactions and induces structural changes forming bilayer like patches of DEEDMAC decorated PAM on the mica surface. Another possibility for the initiation of the structural change of the bilayer could be due to the hydrophobically driven attachment of the PAM to the defects in the bilayer. The patches were not observed when the mica surface was scanned in 0.5 wt % PAM without the DEEDMAC bilayers. To further understand the bilayer structural changes in the presence of PAM, LB technique was used to understand the mechanism of adsorption of PAM with the DEEDMAC head groups.

### Langmuir–Blodgett (LB) trough

The adsorption of PAM to the DEEDMAC monolayer spread at the air–water interface was studied in a LB trough. Isotherms (surface pressure,  $\Pi$  vs. trough area,  $A$ ) of the DEEDMAC surfactant were measured on a clean DEEDMAC monolayer spread at the air–water interface with the sub-phase at 4.5 mM CaCl<sub>2</sub> and pH 4. The DEEDMAC isotherm in the absence of PAM showed that the head group area of the surfactant molecule is  $a_0 \sim 55 \text{ \AA}^2$  at a surface pressure,  $\Pi = 42 \text{ mN m}^{-1}$  (Fig. S1†). The adsorption kinetics of the PAM to the DEEDMAC monolayer was studied qualitatively by maintaining a constant surface pressure at the air–water interface. The DEEDMAC monolayer showed  $\Pi = 42 \text{ mN m}^{-1}$  at a trough area of  $\sim 540 \text{ cm}^2$  (Fig. 6a). Addition of PAM caused the area of the trough to initially decrease in order to maintain  $\Pi$  at  $42 \text{ mN m}^{-1}$ , suggesting that some of the DEEDMAC molecules at the air–water interface were solubilized by PAM. After the initial decrease,  $\Pi$  increased with time due to the slow adsorption of the PAM at the air–water interface from the sub-phase and hence the area of the trough expands slowly to reach an equilibrium value after  $\sim 48 \text{ h}$  in order to maintain  $\Pi = 42 \text{ mN m}^{-1}$  (Fig. 6a).

Isotherms of the DEEDMAC monolayer with adsorbed PAM after the system equilibrated (48 h) showed a phase transition

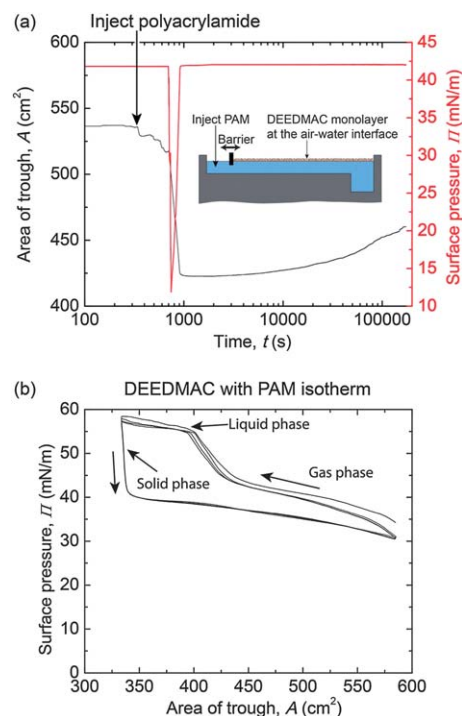


**Fig. 6** (a)  $A$ - $t$  plot for constant surface pressure ( $42 \text{ mN m}^{-1}$ ) that shows the effect of polyacrylamide (PAM) on DEEDMAC monolayer at the air–water interface. PAM micellizes some of the DEEDMAC, hence the trough area  $A$  decreases to maintain the surface pressure constant. (b)  $\Pi$ - $A$  isotherm of the DEEDMAC surfactant with the adsorbed PAM at the air–water interface after  $\sim 48 \text{ h}$  of equilibration.

from gas like to solid like phase behavior (Fig. 6b). The surface pressure never went to zero and the isotherm showed large hysteresis. The isotherms were reproducible for every cycle indicating that the polymer is not squeezed out of the air–water interface once the system has equilibrated. Polyacrylamide (PAM) by itself is not surface active. Adsorption of PAM to the defect-free monolayer at the air–water interface indicates that it preferentially incorporates into the hydrophobic domains of the DEEDMAC monolayer adsorbed at the air–water interface, and that adsorption to defect sites as discussed above (AFM section) is not necessarily the main driving force for PAM adsorption at the supported bilayer interfaces. Most likely some of the DEEDMAC molecules are dissolved from the air–water interface into the bulk of the solution.

## Conclusions

Direct force measurements between two supported DEEDMAC bilayers show that the decay lengths of the double layer forces are greater than the theoretical Debye lengths when the bilayers approach dynamically because the interaction is charge regulated and is closer to constant charge double layer interaction. Charge regulation depends on the rate of approach (and separation) of the surfaces. Fast approach does not allow enough time for equilibration of the counterions on the bilayer surfaces and hence the measured forces are greater than those expected for quasi-statically.<sup>19</sup>

Addition of the PAM causes the hydrophobic backbone of PAM to insert into the interior of the bilayers where it interdigitates with the surfactant tails resulting in the formation of bilayer-like patches of DEEDMAC decorated PAM on the mica surface. The forces between the PAM–bilayers are long ranged and weakly attractive showing signatures of bridging forces. These results show that polymers with hydrophobic backbone can cause instabilities in vesicle dispersions and influence the rheological properties of the dispersion through bridging forces and by inducing structural changes to liposomes, micelles, and supported bilayer membranes.

## Acknowledgements

We acknowledge Procter & Gamble Co. for the materials and funding that made this research possible. The AFM measurements were done in the MRL Central Facilities. The MRL Central Facilities are supported by the MRSEC Program of the NSF under Award no. DMR 1121053; a member of the NSF-funded Materials Research Facilities Network (<http://www.mrfn.org>).

## References

- 1 E. Sackmann, *Science*, 1996, **271**, 43–48.
- 2 S. G. Boxer, *Curr. Opin. Chem. Biol.*, 2000, **4**, 704–709.
- 3 B. A. Cornell, V. L. B. BraachMaksyvtis, L. G. King, P. D. J. Osman, B. Raguse, L. Wiczorek and R. J. Pace, *Nature*, 1997, **387**, 580–583.
- 4 C. Bieri, O. P. Ernst, S. Heyse, K. P. Hofmann and H. Vogel, *Nat. Biotechnol.*, 1999, **17**, 1105–1108.
- 5 C. A. Helm, W. Knoll and J. N. Israelachvili, *Proc. Natl. Acad. Sci. U. S. A.*, 1991, **88**, 8169–8173.
- 6 C. A. Helm and J. N. Israelachvili, *Makromol. Chem., Macromol. Symp.*, 1991, **46**, 433–437.
- 7 L. K. Tamm and H. M. McConnell, *Biophys. J.*, 1985, **47**, 105–113.
- 8 T. A. Harroun, W. T. Heller, T. M. Weiss, L. Yang and H. W. Huang, *Biophys. J.*, 1999, **76**, 937–945.
- 9 H. Schroder, *J. Chem. Phys.*, 1977, **67**, 1617–1619.
- 10 B. A. Lewis and D. M. Engelman, *J. Mol. Biol.*, 1983, **166**, 203–210.
- 11 T. H. Anderson, Y. J. Min, K. L. Weirich, H. B. Zeng, D. Fygenon and J. N. Israelachvili, *Langmuir*, 2009, **25**, 6997–7005.
- 12 E. Reimhult, F. Hook and B. Kasemo, *Langmuir*, 2003, **19**, 1681–1691.
- 13 E. Reimhult, F. Hook and B. Kasemo, *J. Chem. Phys.*, 2002, **117**, 7401–7404.
- 14 A. A. Brian and H. M. McConnell, *Proc. Natl. Acad. Sci. U. S. A.*, 1984, **81**, 6159–6163.
- 15 C. A. Keller, K. Glasmaster, V. P. Zhdanov and B. Kasemo, *Phys. Rev. Lett.*, 2000, **84**, 5443–5446.
- 16 C. A. Keller and B. Kasemo, *Biophys. J.*, 1998, **75**, 1397–1402.
- 17 J. Marra and J. N. Israelachvili, *Biochemistry*, 1985, **24**, 4608–4618.
- 18 R. G. Horn, J. N. Israelachvili, J. Marra, V. A. Parsegian and R. P. Rand, *Biophys. J.*, 1988, **54**, 1185–1186.
- 19 T. H. Anderson, S. H. Donaldson, H. Zeng and J. N. Israelachvili, *Langmuir*, 2010, **26**, 14458–14465.
- 20 A. Ramachandran, T. H. Anderson, L. G. Leal and J. N. Israelachvili, *Langmuir*, 2011, **27**, 59–73.
- 21 J. F. Joanny, L. Leibler and P. G. DeGennes, *J. Polym. Sci., Part B: Polym. Phys.*, 1979, **17**, 1073–1084.
- 22 C. Prestidge and T. F. Tadros, *Colloids Surf.*, 1988, **31**, 325–346.
- 23 W. Liang, T. F. Tadros and P. F. Luckham, *J. Colloid Interface Sci.*, 1993, **158**, 152–158.
- 24 S. Asakura and F. Oosawa, *J. Polym. Sci.*, 1958, **33**, 183–192.
- 25 S. Asakura and F. Oosawa, *J. Chem. Phys.*, 1954, **22**, 1255–1256.
- 26 F. M. Thakkar and K. G. Ayappa, *J. Chem. Phys.*, 2011, **135**, 104901–104914.
- 27 R. M. Pashley and J. N. Israelachvili, *J. Colloid Interface Sci.*, 1984, **97**, 446–455.
- 28 J. Israelachvili, Y. Min, M. Akbulut, A. Alig, G. Carver, W. Greene, K. Kristiansen, E. Meyer, N. Pesika, K. Rosenberg and H. Zeng, *Rep. Prog. Phys.*, 2010, **73**, 036601.
- 29 J. N. Israelachvili, *Intermolecular and surface forces*, Academic Press, Burlington, Mass., 3rd edn, 2011.
- 30 R. Hogg, T. W. Healy and D. W. Fuerstenau, *Trans. Faraday Soc.*, 1966, **62**, 1638–1651.
- 31 G. R. Wiese and T. W. Healy, *Trans. Faraday Soc.*, 1970, **66**, 490–499.
- 32 H. K. Tsao and Y. J. Sheng, *J. Colloid Interface Sci.*, 2001, **233**, 124–130.
- 33 D. McCormack, S. L. Carnie and D. Y. C. Chan, *J. Colloid Interface Sci.*, 1995, **169**, 177–196.
- 34 M. Ruths, H. Yoshizawa, L. J. Fetters and J. N. Israelachvili, *Macromolecules*, 1996, **29**, 7193–7203.
- 35 M. Ruths, J. N. Israelachvili and H. J. Ploehn, *Macromolecules*, 1997, **30**, 3329–3339.
- 36 E. E. Meyer, Q. Lin, T. Hassenkam, E. Oroudjev and J. N. Israelachvili, *Proc. Natl. Acad. Sci. U. S. A.*, 2005, **102**, 6839–6842.